Examination of the effect of differential molecular diffusion in DNS of turbulent non-premixed flames

Chao Han[a], David O. Lignell[b], Evatt R. Hawkes[c], Jacqueline H. Chen[d], Haifeng Wang[a,*]

[a]*School of Aeronautics and Astronautics, Purdue University, West Lafayette, IN 47907, USA*
[b]*Deparment of Chemical Engineering, Brigham Young University, Provo, UT 84602, Unites States*
[c]*School of Mechanical and Manufacturing Engineering, University of New South Wales, Sydney, NSW 2052, Australia*
[d]*Reacting Flow Research Department, Combustion Research Facility, Sandia National Laboratories, Livermore, CA 94551, United States*

Abstract

The effect of differential molecular diffusion (DMD) in turbulent non-premixed flames is studied by examining two previously reported DNS of temporally evolving planar jet flames, one with CO/H_2 as the fuel and the other with C_2H_4 as the fuel. The effect of DMD in the CO/H_2 DNS flames in which H_2 is part of fuel is found to behave similar to laminar flamelet, while in the C_2H_4 DNS flames in which H_2 is not present in the fuel it is simialar to laminar flamelet in early stages but becomes different from laminar flamelet later. The scaling of the effect of DMD with respect to the Reynolds number Re is investigated in the CO/H_2 DNS flames, and an evident power law scaling ($\sim Re^{-a}$ with a a positive constant) is observed. The scaling of the effect of DMD with respect to the Damköhler number Da is explored in both laminar counter-flow jet C_2H_4 diffusion flames and the C_2H_4 DNS flames. A power law scaling ($\sim Da^a$ with a a positive constant) is clearly demonstrated for C_2H_4 nonpremixed flames.

Keywords: Differential molecular diffusion, Turbulent non-premixed flames, Reynolds number, Damköhler number, Laminar flamelet

*Corresponding author. Fax: +1 (607) 255 1222.
Email address: haifeng@purdue.edu (Haifeng Wang)

1. Introduction

Turbulent non-premixed combustion [1] is predominantly controlled by diffusion. An optimal diffusion between fuel and oxidizer can lead to desired combustion with optimal performance in many practical applications. It is therefore important to understand the detailed diffusion process in turbulent non-premixed combustion.

In a turbulent non-premixed flame, there are two fundamental diffusion mechanisms involved to yield large-scale transport of species and energy: molecular diffusion and so-called turbulent diffusion. Molecular diffusion is the result of random motion and collision of molecules. It occurs at the scale of the molecular mean free path. Turbulent diffusion is caused by turbulent eddies which can transport species and energy over a longer distance than molecular diffusion.

Over the past few decades, in Reynolds averaged Navier-Stokes (RANS) simulations [2] and large eddy simulations (LES) [2] of turbulent non-premixed combustion, the study of diffusion has mainly focused on turbulent diffusion [2, 3]. Simple molecular diffusion models including equal-diffusivity and unity Lewis numbers are often assumed in many existing models such as the flamelet [4] and the transported probability density function (PDF) [3] approaches. Molecular diffusion itself is well understood and can be accurately described by using models such as mixture-averaged diffusion or multicomponent diffusion [5]. The modeling of differential molecular diffusion (DMD) in turbulent combustion remains a challenge. Incorporating detailed molecular diffusion treatment in existing turbulent combustion models is non-trivial since many existing turbulent combustion models do not transport species and energy directly due to the closure problem associated with the highly nonlinear reaction source terms. For example, in flamelet models, the effect of multi-component species and energy transport has to be incorporated by relating the scalars to a few tracing scalars such as mixture fraction. For several decades, the assumption of equal-diffusion has been used in flamelet models. Extending the flamelet models and other models to account for DMD is not trivial. The purpose of the present study is to provide critical understanding of the effect of DMD to assist future work of incorporating DMD in existing turbulent combustion

models, including flamelet models. For this purpose, a molecular diffusion description based on mixture-averaged diffusion has been used. Mixture-averaged diffusion is generally viewed as adequate for simple cases that are studied in this work [6, 7]. An important species in discussing DMD is H_2 because of its low Lewis number, $Le_{H2} \sim 0.32$. H_2 is an intermediate species from combustion of hydrocarbon fuels. It can also be an addition to other fuels [8]. The presence of H_2 in fuel and its production during chemical reaction complicate the effect of DMD and a clear understanding of DMD under the different situations is required for its accurate modeling.

Some arguments have been used in the past to support the highly simplified molecular diffusion models used in turbulent combustion modeling. In the context of Reynolds averaging [2], the effect of molecular diffusion is often neglected or highly simplified, based on the argument that the turbulent diffusion dominates molecular diffusion in a high Reynolds number (Re) flow [2, 9, 10]. We can introduce a nominal molecular diffusivity D_M to quantify molecular diffusion and a turbulent diffusivity D_T to quantify turbulent diffusion. A scaling analysis [9, 10] shows that D_M/D_T scales as Re^{-1}, i.e., $D_T \gg D_M$ for high Re problems. For highly turbulent non-reacting flows, the effect of molecular diffusion is expected to be insignificant in comparison to turbulent diffusion (in the context of Reynolds averaging).

However, there are many cases in which molecular diffusion can have substantial effects. In turbulent premixed combustion, the significance of detailed molecular diffusion has been widely recognized [11–15]. In turbulent non-premixed combustion, chemical reaction occurs at the molecular scale, and thus how the reactants are brought together at the molecular scale directly determines the chemical pathways. Fundamentally, it is molecular diffusion that ultimately mixes reactants at the molecular scale. Thus, molecular diffusion has non-negligible theoretical significance in turbulent non-premixed combustion. Moreover, based on the Reynolds averaging argument, locally low Re can be frequently encountered in turbulent non-premixed combustion, such as a lowered Re in high temperature flame regions [16], and locally weak turbulence or laminar regions [17]. Furthermore, in the context of LES, the magnitude of molecular diffusivity can be comparable to the sub-filter scale turbulent diffusivity [18]. Based on these considerations, the effect of molecular diffusion in

turbulent non-premixed combustion cannot be viewed as universally insignificant. A quantitative understanding of the effect of molecular diffusion and its interaction with turbulent diffusion and chemical reaction is needed to provide a detailed understanding of turbulent non-premixed combustion.

DMD is a phenomenon resulting from the different rates of molecular diffusion of different species. The significance of DMD has been reported in many previous studies (e.g. [10, 19–28]). In this work, we focus on examining the effect of DMD in two Sandia DNS of temporally evolving planar jet flames: CO/H_2 non-premixed flames [29] and C_2H_4 flames [30], with the goal to provide a quantitative understanding of the DMD effect in these two different flames and the difference of the two flames in terms of the DMD effect. The CO/H_2 DNS flame series contain three cases with fixed Damköhler number Da and different Re, and the C_2H_4 DNS flame series contain three cases with different Da and fixed Re, as shown in Table 1. These DNS flames provide accessible information for studying the effect of DMD in turbulent non-premixed combustion. Specifically, in this work, we have three objectives:

1. Conduct comparative studies of the effect of DMD in steady laminar diffusion flames and in the two DNS flames to provide understanding of the difference of the effect of DMD in these two DNS flames;

2. Examine the effect of Re on DMD in the CO/H_2 DNS flames and perform scaling analysis for the effect of DMD with respect to Re;

3. Examine the effect of Da number on DMD in steady laminar diffusion flames and in the C_2H_4 DNS flames, and perform scaling analysis for the effect of DMD with respect to Da.

The remainder of the paper is organized as follows. Section 2 interrogates the datasets of the two DNS flames to examine the characteristic differences of the effect of DMD in them. To assist the examination, we use steady laminar diffusion flamelets as the reference of the effect of DMD. Section 3 investigates the dependence of the effect of DMD against Re in the CO/H_2 DNS flames and analyzes the scaling of the effect of DMD against Re. Section

4 studies the dependence of the effect of DMD on Da in the C_2H_4 DNS flames. Scaling analysis of the effect of DMD against Da is performed in both C_2H_4 laminar diffusion flamelets (Section 4.2) and the C_2H_4 DNS flames (Section 4.3). Conclusions are drawn in Section 5.

2. Differential molecular diffusion in DNS flames

2.1. Temporally evolving DNS flames

The datasets from DNS of two temporally evolving planar jet flames from the previous work [29, 30] are employed for the study of the effect of DMD in this work. One flame uses CO/H_2 as the fuel [29], and the other flame uses C_2H_4 as the fuel [30]. Three cases are considered in the CO/H_2 DNS flames, case L, case M, and case H, with increasing Re and with the same Da as shown in Table 1. These cases provide an excellent test case to examine and to quantify the effect of Re on DMD. The C_2H_4 DNS flames have three cases as well, case 1, case 2, and case 3, with decreasing Da and with the same Re, which is ideal for the exploration of the effect of Da on DMD. In addition to the study of the effect of Re and Da on DMD, we will also compare the effect of DMD in these two different sets of DNS flames, with the focus on the effect of the existence of H_2 in the fuel on DMD.

Table 1: Summary of the conditions for the CO/H_2 and C_2H_4 DNS flames.

	CO/H_2 DNS flames			C_2H_4 DNS flames		
	case L	case M	case H	case 1	case 2	case 3
Re	2510	4478	9079	5120	5120	5120
Da	0.011	0.011	0.011	0.023	0.017	0.011

In the DNS flames, the initial conditions for the simulations are specified from a steady flamelet solution with equal molecular diffusivity and unity Lewis number. It appears that the effect of the equal-diffusivity initial condition fades very quickly in time in the DNS flames, which is discussed later.

2.2. Quantification of the effect of differential molecular diffusion

Quantification of the effect of DMD in turbulent combustion is a difficult task, and so far there is no widely accepted quantification approach. From the perspective of modeling the effect of DMD in turbulent combustion, the following sets of criteria can be used to assess a quantification approach for the effect of DMD.

(a) Representation of DMD as directly as possible.

(b) Simple formulation for easy use in both experiments and simulations.

(c) Measurable from the experiments for a direct model validation.

(d) Quantifiable from the common turbulent combustion models that can be used for comparison with experiments for a model validation.

In this work, we adopt a simple quantification introduced by Bilger [9]. To quantify the effect of DMD in the DNS flames, we first define mixture fraction ξ_α based on an element α as

$$\xi_\alpha = \frac{Y_\alpha - Y_{\alpha,o}}{Y_{\alpha,f} - Y_{\alpha,o}}, \tag{1}$$

where Y_α, $Y_{\alpha,f}$ and $Y_{\alpha,o}$ are the mass fractions of element α in the local gas mixture, in the fuel, and in the oxidizer, respectively.

For laminar flames, the effect of DMD can be quantified by the difference, $z_{\alpha\beta}$, of different mixture fractions defined based on different elements [9, 10, 31],

$$z_{\alpha\beta} = \xi_\alpha - \xi_\beta. \tag{2}$$

In the above definition in equation (2), $z_{\alpha\beta}$ is defined locally at each point and time for a given flame. It is noted that ξ_α and ξ_β at the same point and time inside the same flame are not independent. Thus $z_{\alpha\beta}$ can be viewed as a function of ξ_β at a fixed point and time in a flame. A global parameter, $Z_{\alpha\beta}$, is defined to provide an average assessment of the effect of DMD of the entire flame,

$$Z_{\alpha\beta} = \sqrt{\frac{1}{\xi_{\beta,max}} \int_0^{\xi_{\beta,max}} z_{\alpha\beta}^2 d\xi_\beta}, \tag{3}$$

in which, $\xi_{\beta,max}$ is the maximum possible value of ξ_β ($\xi_{\beta,max} \leq 1$). The parameter $Z_{\alpha\beta}$ can be viewed as the square root of the weighted average of $z^2_{\alpha\beta}$ based on the occupied volume of $z^2_{\alpha\beta}$ in the mixture fraction ξ_β space, and it is introduced purely for the purpose of enabling a global quantification of the effect of DMD for a flame to facilitate the later studies on the effect of Re and Da on DMD. No symmetric condition is imposed on the definition of $Z_{\alpha\beta}$, i.e., $Z_{\alpha\beta} \neq Z_{\beta\alpha}$.

For turbulent flames, we can introduce Favre averaging and define the corresponding Favre averaged quantities to provide a statistical quantification of the effect of DMD in the turbulent non-premixed flames, $\tilde{z}_{\alpha\beta}$, and $\widetilde{Z}_{\alpha\beta}$,

$$\tilde{z}_{\alpha\beta} = \tilde{\xi}_\alpha - \tilde{\xi}_\beta, \tag{4}$$

$$\widetilde{Z}_{\alpha\beta} = \sqrt{\frac{1}{\tilde{\xi}_{\beta,max}} \int_0^{\tilde{\xi}_{\beta,max}} \tilde{z}^2_{\alpha\beta} d\tilde{\xi}_\beta}, \tag{5}$$

where "$\sim$" denotes Favre averaging. Similarly, we can define the root mean square (rms) quantities to measure the effect of DMD as,

$$z''_{\alpha\beta} = \sqrt{\widetilde{z^2_{\alpha\beta}} - \tilde{z}^2_{\alpha\beta}}, \tag{6}$$

$$Z''_{\alpha\beta} = \sqrt{\frac{1}{\tilde{\xi}_{\beta,max}} \int_0^{\tilde{\xi}_{\beta,max}} (z''_{\alpha\beta})^2 d\tilde{\xi}_\beta}. \tag{7}$$

Different elements can be used to define the above parameters. In combustion problems, hydrocarbon fuels are most commonly used. In this work, we use the elements H and C to define the above parameters, z_{HC}, Z_{HC}, $\tilde{z}_{HC}$, $\widetilde{Z}_{HC}$, z''_{HC}, and Z''_{HC}, to quantify the effect of DMD. To show that z_{HC} is representative, we compare the values of different $z_{\alpha\beta}$ based on the different elements in the OPPDIF calculations [32] of the opposed laminar jet flames in Figure 1. From the figure, we see two types of variations of $z_{\alpha\beta}$ against ξ_C. One shows that there is a single change of sign of $z_{\alpha\beta}$ inside the mixture fraction space, excluding the boundaries, and the profile of z_{HC} from the CO/H_2 flame is a typical example. The other shows two sign changes of $z_{\alpha\beta}$, and the profile of z_{HC} from the C_2H_4 flame is a typical example. In terms of the magnitudes, we can see that z_{HC} represents all $z_{\alpha\beta}$ well. Thus

z_{HC} is a good representation of the effect of DMD presented in both DNS flames. It is mentioned above that Z_{HC} is not symmetric, $Z_{HC} \neq Z_{CH}$. The relative difference between Z_{HC} and Z_{CH} is very small (about 2%) in the two DNS flames. Therefore the quantification parameters for the effect of DMD based on the elements H and C used in this paper are representative of the parameters based on all the other elements.

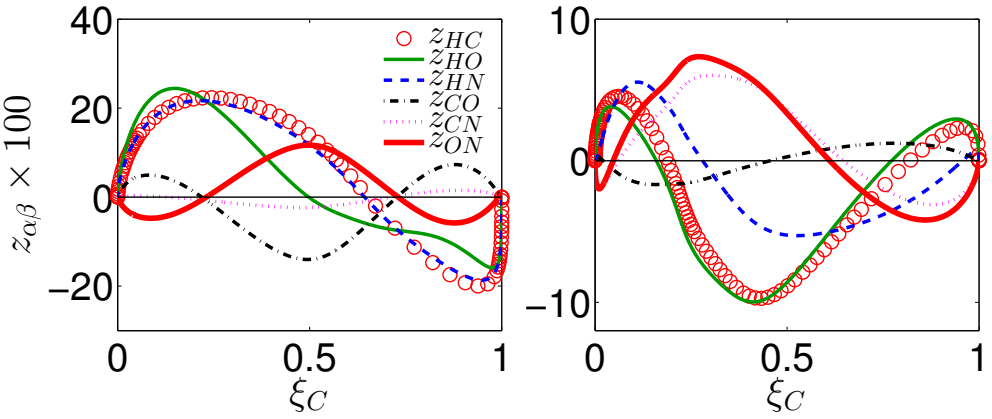

Figure 1: The values of $z_{\alpha\beta}$ based on the different elements against ξ_C in the OPPDIF calculations of the opposed laminar jet flames with the same boundary conditions as the CO/H_2 DNS flames (left) and the C_2H_4 DNS flame case 1 (right). The strain rate of the OPPDIF calculation is set to be 100 s^{-1}.

The above quantification method of the effect of DMD based on $z_{\alpha\beta}$ in equation (2) has been widely used in the past three decades for the study of DMD (e.g., [9, 10, 21, 22, 31, 33–38]). It satisfies all (a)-(d) criteria mentioned above for assessing a DMD quantification approach. There are other methods available to quantify the effect of DMD. Sutherland et al. [20] quantifies DMD by the source term of mixture fraction equations that are written based on element mass fractions. Any non-zero value of the source term is the result of the DMD. This approach is similar to the approach in equation (2) in the sense that both represent a lumped effect of DMD rather than the direct effect of DMD between any two species. The approach by Sutherland et al. [20] is not adopted in the present study due to measurement and modeling challenges, i.e., the lack of aforementioned properties, (b)-(d).

In this work, the molecular diffusion is described by using the mixture-averaged formulation with thermal diffusion (TD) neglected. This is the choice made in the DNS flames

[29, 30]. The accuracy of the mixture-averaged formulation is examined in the OPPDIF [32] calculations of the opposed jet flames with the boundary conditions from the two DNS flames, as shown in Figure 2. From the figure, we can see that the mixture-averaged diffusion and the multicomponent diffusion (with or without TD) yield almost identical results for z_{HC} (relative difference within 1.5%). The small difference between the mixture-averaged diffusion and the multicomponent diffusion is also reported in the DNS study in [7]. TD is neglected in this work following the DNS [29, 30], and this yields about 25% error for z_{HC} in the laminar CO/H_2 flame and 20% in the laminar C_2H_4 flame, as shown in Figure 2.

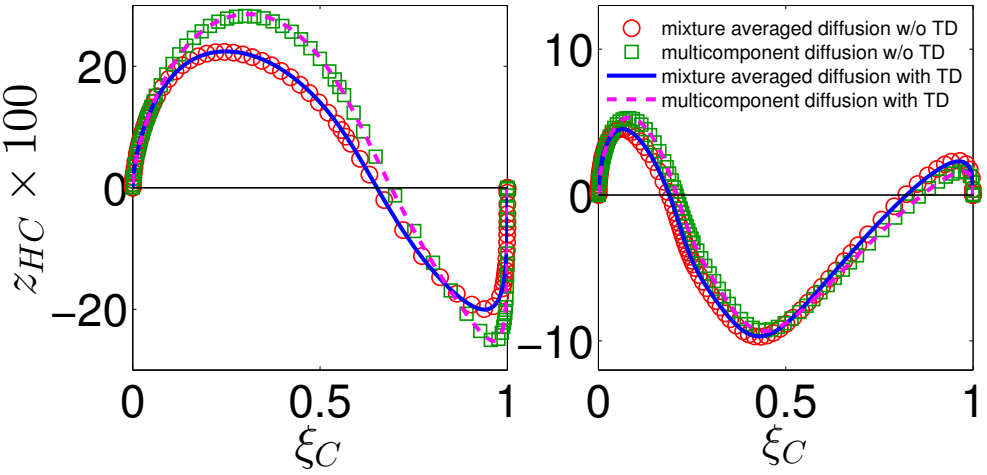

Figure 2: The values of z_{HC} against ξ_C in the OPPDIF calculations of the opposed laminar jet flames with different descriptions of molecular diffusion and with the same boundary conditions as the CO/H_2 DNS flames (left) and the C_2H_4 DNS flame case 1 (right). The strain rate of the OPPDIF calculation is set to be 100 s^{-1}.

2.3. Quantification of species contributions to differential molecular diffusion

Although z_{HC} from Section 2.2 represents a lumped effect of DMD, the contribution of each species to z_{HC} can be precisely quantified, given that such a contribution is also known for the case of equal diffusivity.

The element mass fraction Y_α is related to species mass fractions as,

$$Y_\alpha = \sum_{k=1}^{n_s} \frac{n_{\alpha,k} w_\alpha}{w_k} Y_k, \tag{8}$$

where n_s is the number of species in a combustion system, $n_{\alpha,k}$ is the number of element α in the k-th species, w_α is the atomic weight of α, w_k is the molecular weight of the k-th species, and Y_k is the mass fraction of the k-th species. Substituting equation (8) into (1) and using (2), we obtain,

$$z_{\alpha\beta} = \sum_{k=1}^{n_s} \hat{z}_{\alpha\beta,k}, \tag{9}$$

with

$$\hat{z}_{\alpha\beta,k} = (c_{\alpha,k} + c_{\beta,k}) \cdot (Y_k - Y_{k,o}), \tag{10}$$

$$c_{\alpha,k} = \frac{\hat{c}_{\alpha,k}}{\sum_{j=1}^{n_s} \hat{c}_{\alpha,j}(Y_{j,f} - Y_{j,o})}, \tag{11}$$

$$\hat{c}_{\alpha,k} = \frac{n_{\alpha,k} w_\alpha}{w_k}. \tag{12}$$

The value of $\hat{z}_{\alpha\beta,k}$ in equation (10) describes the contribution of species k to the DMD parameter $z_{\alpha\beta}$. This value, however, does not describe the sole contribution of species k to DMD since even if equal diffusivity is assumed, $\hat{z}_{\alpha\beta,k}$ is not zero because of reaction and transport. If we subtract the value of $\hat{z}_{\alpha\beta,k}$ by $\hat{z}^{ED}_{\alpha\beta,k}$ corresponding to the case of equal diffusivity, we then obtain the contribution of species k to DMD that excludes the effect of reaction and transport, which we denote as $\zeta_{\alpha\beta,k}$,

$$\zeta_{\alpha\beta,k} = \hat{z}_{\alpha\beta,k} - \hat{z}^{ED}_{\alpha\beta,k}. \tag{13}$$

Obviously, $\sum_{k=1}^{n_s} \hat{z}^{ED}_{\alpha\beta,k} = 0$, which leads to, when combined with (9) and (13),

$$z_{\alpha\beta} = \sum_{k=1}^{n_s} \zeta_{\alpha\beta,k}. \tag{14}$$

The contributions of species to the DMD parameter $z_{\alpha\beta}$ can thus be precisely quantified by $\zeta_{\alpha\beta,k}$ which becomes zero when there is no effect of DMD, i.e., assuming equal diffusivity.

The species contributions to DMD are examined in the laminar flamelet solutions corresponding to the DNS boundary conditions. Here again we use elements H and C to examine

the contributions $\zeta_{HC,k}$, which sum to $z_{HC} = \sum_{k=1}^{n_s} \zeta_{HC,k}$ in the laminar flamelet solutions. Two OPPDIF calculations [32] are conducted for each DNS condition with the same strain rate a_s =100 s^{-1} to obtain $\hat{z}_{HC,k}$ and $\hat{z}_{HC,k}^{ED}$ in (10), in order to compute $\zeta_{HC,k}$ in (13).

The results of $\zeta_{HC,k}$ are shown in Figure 3 for the two DNS flame conditions. For the CO/H_2 DNS flame condition, only the first six species that have the largest contributions to DMD are shown, and the primary contribution to DMD is seen to be caused by only two species, H_2O and H_2. The contribution of H_2O dominates in the range of $\xi_C < 0.65$, while the contribution of H_2 dominates in the range of $\xi_C > 0.65$. The species H_2O, which has a Lewis number around 0.9 that is not very different from unity, can cause the DMD on a similar order of magnitude to the light species H_2 in the CO/H_2 flame. In the C_2H_4 flame, the first eight species with the largest contributions to DMD are shown. In the range of $\xi_C < 0.2$, the contribution of H_2O dominates all other species. For $\xi_C > 0.2$, five species have the most significant contributions to DMD, and they are H_2, C_2H_2, CO, CO_2, and H_2O. The contributions from CO and CO_2 are in a opposite sign, and cancel each other significantly; the contribution of C_2H_2 is surprisingly large (even though the Lewis number of C_2H_2 is around 1.2 that is not far from unity) and is negative; the contribution of H_2O is negative for $0.2 < \xi_C < 0.65$ and positive for $\xi_C > 0.65$; and the contribution of H_2 is the most significant among all species, which peaks at about $\xi_C \approx 0.4$, is negative in $0.2 < \xi_C < 0.8$, and is positive in $\xi_C > 0.8$. Comparing the CO/H_2 flame and the C_2H_4 flame, we can see that the contribution of H_2 to DMD peaks near the location where H_2 is approximately maximum. For the CO/H_2 flame, this maximum occurs at the fuel boundary and is away from the reaction front, while for the C_2H_4 flame, the H_2 is produced during reaction and reaches maximum near the flame front.

As discussed above, the species contributions to the DMD parameter $z_{\alpha\beta}$ can be quantified precisely. A drawback of this quantification is that it requires the corresponding results with equal diffusivity, which significantly limits the approach. In the DNS flames studied in this work, the results with equal diffusivity are not available and we will not be able to quantify the contribution of each species to the DMD parameter in those flames. In the following discussions, we will mainly focus on the lumped effect of DMD in terms of z_{HC} in

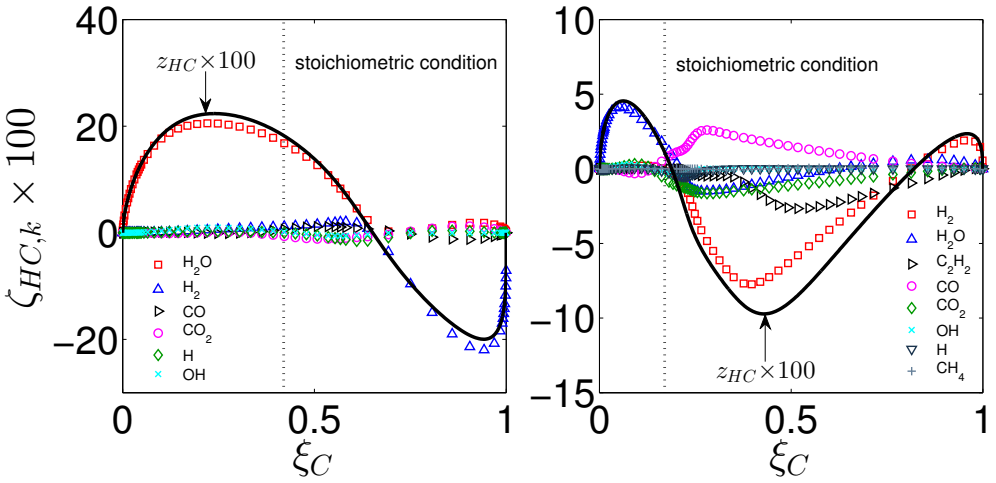

Figure 3: The values of $\zeta_{HC,k}$ against ξ_C in the OPPDIF calculations of the opposed laminar jet flames with the same boundary conditions as the CO/H_2 DNS flames (left) and the C_2H_4 DNS flame case 1 (right). The strain rate of the OPPDIF calculation is set to be 100 s^{-1}. For reference, the value of z_{HC} is also shown as solid lines. The stoichiometric condition is shown as the vertical dotted lines.

the DNS flames.

2.4. Differential molecular diffusion in flamelet as the reference

To interrogate the effect of DMD in the DNS flames, we use the DMD effect observed in a laminar flamelet as a reference case. Examining the similarity and difference between the effect of DMD in DNS and in the reference flamelet can help identify the different behaviors of the effect of DMD in the two DNS flames. The fundamental idea behind flamelet models relies on the similarity of the flame structures in laminar and turbulent flames. If there is such a similarity, it is implied that the turbulent flames can be reasonably modeled by the laminar flamelet models. In this work, we extend this implication to the effect of DMD. The similarity of the effect of DMD in flamelet and in DNS implies that the DMD effect can be captured by using flamelet models. We loosely call this type of DMD effect as flamelet-like. Similarly, if the DMD effect in DNS deviates from that in a flamelet, we call it non-flamelet-like. This categorization is qualitative in nature, and the main purpose is to determine different behaviors of the DMD effect which ultimately can help develop suitable models for the effect of DMD in the RANS or LES modeling of turbulent flames.

The effect of DMD in a flamelet is examined in Figure 4 for the two cases with the boundary conditions the same as the CO/H_2 DNS flame (case L) and the C_2H_4 flame (case 1). The steady flamelet solutions are computed from OPPDIF [32] for opposed laminar jet diffusion flames with the same boundary conditions as the DNS flames and with the strain rate from 1 s^{-1} to the extinction limit. The profiles of z_{HC} in the flamelet can be characterized by the shapes of the profiles and the magnitudes of the profiles. To a large extent, we can see that the shapes of the profiles of the different flamelets with the different strain rates are similar and are not significantly dependent on the strain rate. This provides the basis for the similarity analysis of the DMD effect in DNS flames and in flamelets in the following discussions. The effect of DMD is argued to be similar in DNS flames and in flamelets if the shapes of profiles of z_{HC} or $\tilde{z}_{HC}$ are similar. In the analysis, the magnitudes of z_{HC} or $\tilde{z}_{HC}$ are not relevant because the magnitudes are influenced significantly by Re. The effect of Re on DMD can be incorporated into the flamelet models by following Wang [10]. Thus if the effect of DMD in DNS and flamelets exhibit similar behaviors in terms of the shapes of the profiles of z_{HC} or $\tilde{z}_{HC}$, we expect that the effect of DMD in DNS flames can be captured by flamelet models, as having been demonstrated by the modeling studies of the effect of DMD in turbulent flames [10, 39].

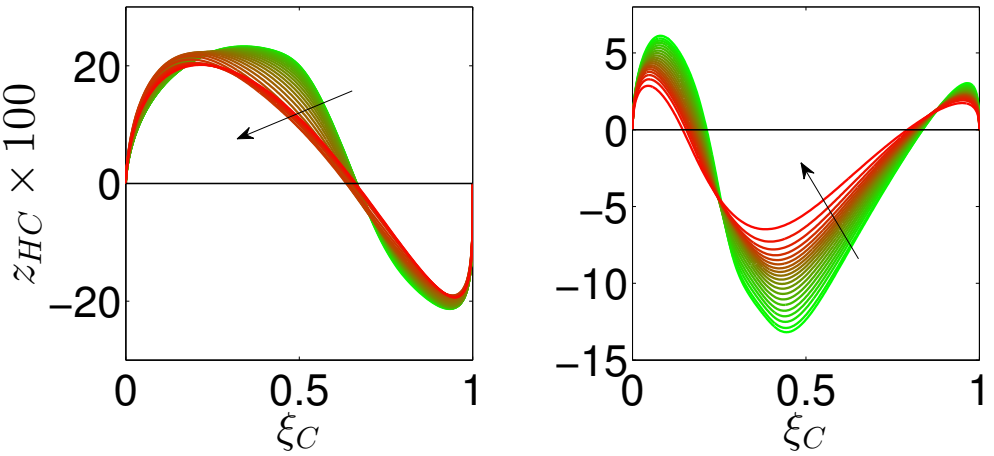

Figure 4: The values of z_{HC} against ξ_C from the steady flamelet solutions with the same boundary conditions as the CO/H_2 DNS flames (left) and the C_2H_4 DNS flame case 1 (right). The arrows indicate the directions of increasing the strain rate of the flamelet.

2.5. Differential molecular diffusion in CO/H_2 DNS flames

Figure 5 shows the temporal evolution of $\widetilde{Z}_{HC}$, Z''_{HC} (defined in equations (5) and (7), respectively) and the burning index BI in the three CO/H_2 DNS flames, case L, case M and case H. The burning index [40] is used to quantify the level of local extinction. It is defined as $BI = \langle T|\xi_{st}\rangle/T_{ref}$, where $\langle T|\xi_{st}\rangle$ is the conditional mean temperature at the stoichiometric condition, and $T_{ref} = 2003$ K is the reference temperature taken to be the temperature at the stoichiometic condition from a flamelet with a_s =100 s^{-1}. At time equal to zero, both $\widetilde{Z}_{HC}$ and Z''_{HC} are identically zero because a steady flamelet solution with unity Lewis number is used as the initial condition in the DNS flames [29, 30]. At an early time ($t/t_j \leq 10$, where t_j is the characteristic flow time scale in the DNS flames [29, 30]), both $\widetilde{Z}_{HC}$ and Z''_{HC} increase in time due to the effect of DMD and reach maximum values between $t/t_j = 5$ and 15. The values of BI in the three flames increase slightly before $t/t_j < 10$, and then decrease rapidly to reach the minimum shortly after $t/t_j = 20$ before increasing again, indicating the increased local extinction followed by re-ignition [40]. Comparing the three flames, the local extinction level increases when the Re increases from flame L, to flame M and then to flame H.

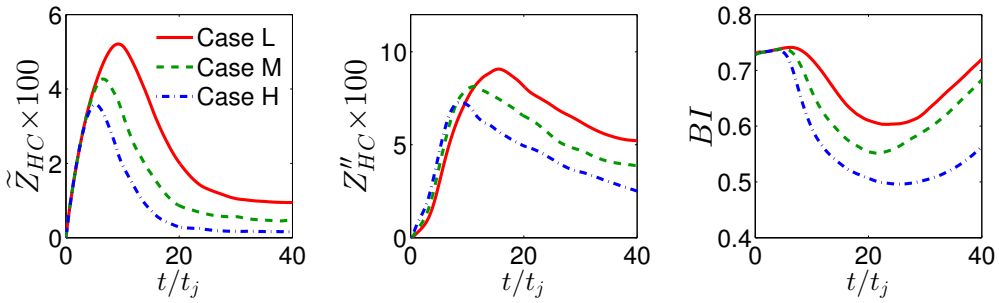

Figure 5: Temporal evolution of $\widetilde{Z}_{HC}$ (defined in equation (5)), Z''_{HC} (defined in equation (7)) and the burning index BI in the three CO/H_2 DNS flames.

Figure 6 shows $\tilde{z}_{HC}$, defined in equation (4), against $\tilde{\xi}_C$ for the three CO/H_2 DNS flames. The lines are the DNS results at the different times $t/t_j = 10$ (solid lines), $t/t_j = 15$ (dashed lines), $t/t_j = 20$ (dash-dotted lines) and $t/t_j = 30$ (dotted lines). The shaded area covers all the steady flamelet solutions shown in Figure 4 that are computed from OPPDIF [32]

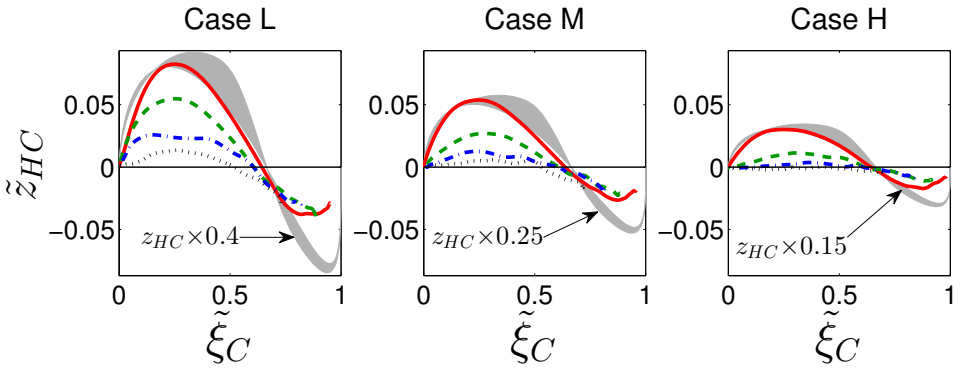

Figure 6: Profiles of $\tilde{z}_{HC}$, defined in equation (4), against $\tilde{\xi}_C$ in the three CO/H_2 DNS flames, case L (left), case M (middle), and case H (right), at $t/t_j = 10$ (solid lines), at $t/t_j = 15$ (dashed lines), at $t/t_j = 20$ (dash-dotted lines), at $t/t_j = 30$ (dotted lines). The shaded area covers the steady flamelet solutions z_{HC}, which are scaled by a factor of 0.4, 0.25 and 0.15, respectively.

for opposed laminar jet diffusion flames with the same boundary conditions as the DNS flames and with the strain rate from 1 s^{-1} to the extinction point at 2500 s^{-1}. The flamelet solutions are scaled by a factor of 0.4, 0.25, and 0.15 for flames L, M, and H, respectively, for an easy comparison with the DNS results. From the flamelet solutions, we can see that z_{HC} is negative when $\xi_C > 0.65$ and is positive when $\xi_C < 0.65$. Light molecules such as H_2 in the fuel diffuse faster than carbon containing species on the fuel rich side, and thus z_{HC} is negative indicating less H_2 compared to the case of equal diffusion. The value of z_{HC} becomes positive away from the fuel side ($\xi_C < 0.65$) because of the combustion product H_2O entering this region as discussed in Figure 3. A characteristic similarity of the effect of DMD between DNS and flamelet solutions can be observed from the figure. Both the DNS and the flamelet solutions yield negative $\tilde{z}_{HC}$ (or z_{HC}) near the fuel side and positive $\tilde{z}_{HC}$ (or z_{HC}) near the oxidizer side, and in both cases, $\tilde{z}_{HC}$ (or z_{HC}) changes sign once at about the same mixture fraction ($\tilde{\xi}_C$ or $\xi_C \approx 0.65$). At $t/t_j = 10$, the profiles of $\tilde{z}_{HC}$ in Figure 6 from the DNS are qualitatively similar to those from a steady flamelet solution. This, along with Figure 5, suggests that the effect of the initial equi-diffusion in the DNS data has faded. The magnitudes of $\tilde{z}_{HC}$ from the DNS and those of z_{HC} from the flamelets are, however, very different and this is attributed to differences between the

three dimensional, unsteady DNS with different levels of local extinction, and the steady one-dimensional flamelets. As discussed in Section 2.4, this magnitude difference is mainly caused by the Re effect, and it was found before that the magintudes of $\tilde{z}_{HC}$ in turbulent non-premixed flames are inversely propportional to Re [9]. As previously noted, the effect of Re on DMD can be incorporated by following the models developed in Wang [10]. The similarity of the shapes of the profiles of z_{HC} and $\tilde{z}_{HC}$ in laminar flamelet and DNS flames determines if the effect of DMD in DNS flames can be captured by flamelet or not, following the discussions in Section 2.4. The similarity of the effect of DMD in the CO/H_2 DNS flames and the laminar flamelets suggests that the effect of DMD in the CO/H_2 DNS flames can probably be captured by flamelet models [4]. We call this type of DMD effect in the CO/H_2 DNS flames "flamelet-like".

2.6. Differential molecular diffusion in C_2H_4 DNS flames

In the C_2H_4 DNS flames, the temporal evolution of $\widetilde{Z}_{HC}$, Z''_{HC} and BI (defined similarly to the CO/H_2 flames in Section 2.5 with T_{ref} = 2526 K, 2425 K, 2284 K, respectively from flamalet solutions) is shown in Figure 7. A similar evolution to that in the CO/H_2 DNS flames in Figure 5 is observed here for $\widetilde{Z}_{HC}$ and Z''_{HC}. The values of $\widetilde{Z}_{HC}$ reach its peak at about $t/t_j = 7.5$. Because of the same reason due to the effect of the equal diffusion initial conditions in the DNS, we consider the DNS results only at $t/t_j \geq 7.5$ in the C_2H_4 flames. The values of BI decrease from the beginning for all three flames, followed by a increase that is observed only in case 1 and case 2 before $t/t_j = 40$. According to Lignell et al. [30], case 3 is almost extinguished after $t/t_j = 30$, followed by stratified premixed flame re-ignition. The severe local extinction in the C_2H_4 flames is expected to interact strongly with DMD. The influence of extinction in case 3 will be noted when encountered in the following discussions.

Figure 8 shows $\tilde{z}_{HC}$ against $\tilde{\xi}_C$ for the three C_2H_4 DNS flames. The lines are the DNS results at the different times $t/t_j = 7.5$ (solid lines), $t/t_j = 10$ (dashed lines), $t/t_j = 20$ (dash-dotted lines) and $t/t_j = 30$ (dotted lines). The shaded area covers all the steady laminar flamelet solutions as shown in Figure 4 with the strain rate from 1 s^{-1} to the extinction points at 7648 s^{-1}, 5803 s^{-1} and 3888 s^{-1}, respectively. The flamelet solutions are scaled

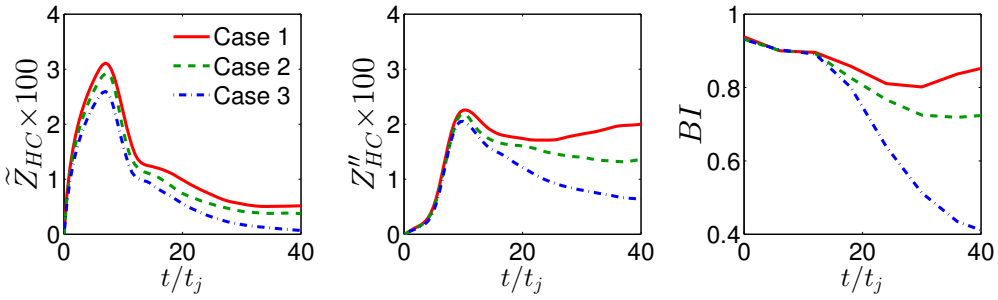

Figure 7: Temporal evolution of $\widetilde{Z}_{HC}$, Z''_{HC} and the burning index BI in the three C_2H_4 DNS flames.

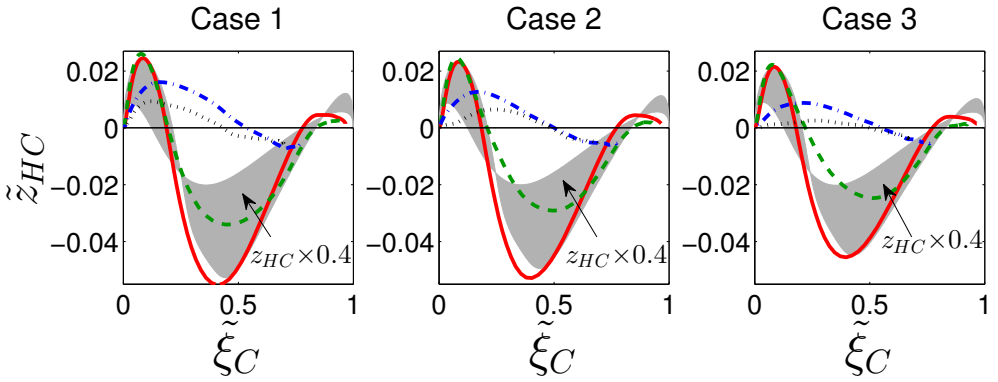

Figure 8: Profiles of $\tilde{z}_{HC}$ against $\tilde{\xi}_C$ in the three C_2H_4 DNS flames, case 1 (left), case 2 (middle), and case 3 (right), at $t/t_j = 7.5$ (solid lines), at $t/t_j = 10$ (dashed lines), at $t/t_j = 20$ (dash-dotted lines), at $t/t_j = 30$ (dotted lines). The shaded area covers the steady flamelet solutions z_{HC}, which are scaled by a factor of 0.4.

by a factor of 0.4 for all three cases (this single factor is consistent with the constant Re in the three cases). Two major characteristic differences of DMD in the C_2H_4 DNS flames can be observed in comparison with the CO/H_2 DNS flames discussed in Section 2.4. First, based on the flamelet solutions in the C_2H_4 flames, we can see that z_{HC} changes sign twice in the mixture fraction space. Positive z_{HC} is observed at conditions with $\xi_C < 0.2$ and $\xi_C > 0.8$, and negative z_{HC} is observed in between. This difference of the effect of DMD in the C_2H_4 DNS flames, when compared to the CO/H_2 DNS flames in Figure 6, has been explained by the role difference of H_2 in the two flames in Section 2.3. The distinct roles of H_2 as a fuel component and as a stable intermediate species apparently result in quite different DMD effect in the CO/H_2 DNS flames and in the C_2H_4 DNS flames [20]. Second,

comparing the C_2H_4 DNS flames and the flamelet solutions in Figure 8, we observe a strong similarity between them in terms of the shape of $\tilde{z}_{HC}$ (or z_{HC}) profiles at $t/t_j \leq 10$. At later times $t/t_j \geq 20$, however, $\tilde{z}_{HC}$ from the DNS flames are qualitatively different than z_{HC} from the flamelet solutions, particularly at the conditions where z_{HC} (or $\tilde{z}_{HC}$) changes sign. The flamelet solutions yield the first sign change of z_{HC} between $\xi_C \in (0.15, 0.21)$, while the DNS yields the first sign change of $\tilde{z}_{HC}$ at a much larger value of $\tilde{\xi}_C > 0.28$ when $t/t_j \geq 20$. This difference indicates the DMD effect in the C_2H_4 DNS flames is different from that in the CO/H_2 DNS flames when the steady laminar flamelet solutions are used as references. As a result, it is expected that the flamelet models [4] are unlikely able to reproduce the effect of DMD in the C_2H_4 DNS flames, following the discussion in Section 2.4. We call this type of DMD effect in the C_2H_4 DNS flames "non-flamelet-like". This imposes additional challenges to the development of DMD models because of the existence of the different types of DMD effect.

In summary, we use the effect of DMD in steady laminar flamlets as a reference to examine the effect of DMD in both the CO/H_2 and C_2H_4 DNS flames. The CO/H_2 DNS flames show flamelet-like DMD effect, while the C_2H_4 DNS flames show, at early times ($t/t_j \leq 10$), flamelet-like DMD effect, but non-flamelet-like at later times. In the following sections, we further examine the effect of Reynolds number Re in Section 3 and Damköhler number Da in Section 4 on DMD.

3. Dependence of differential molecular diffusion on *Re* number

The dependence of the effect of DMD on dimensionless numbers such as Re and Da are useful for a quantitative understanding of the effect of DMD, for determining the scaling of DMD, and for developing new DMD models. In this section, we first examine the dependence of the effect of DMD on Re, by using the CO/H_2 DNS flames in which the effect of Re is isolated since Da is fixed in all three CO/H_2 DNS flames.

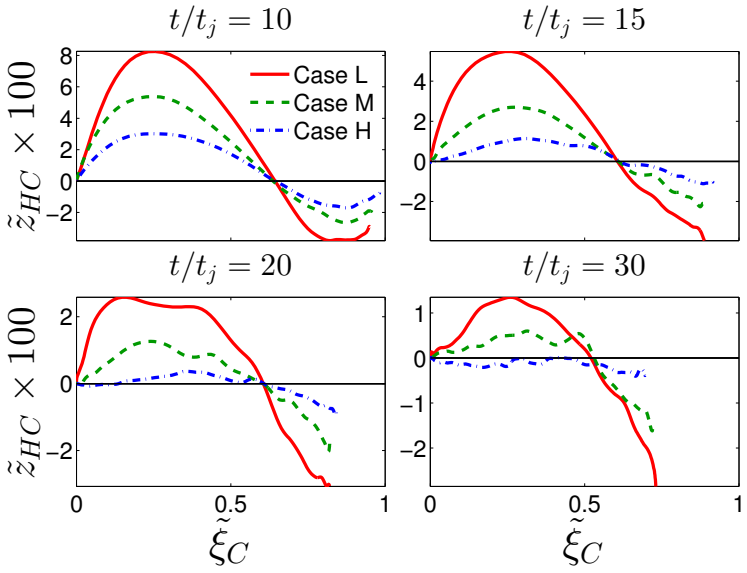

Figure 9: Comparison of $\tilde{z}_{HC}$ against $\tilde{\xi}_C$ in the three CO/H_2 DNS flames, case L (solid lines), case M (dashed lines), and case H (dash-dotted lines), at $t/t_j = 10$, 15, 20, and 30.

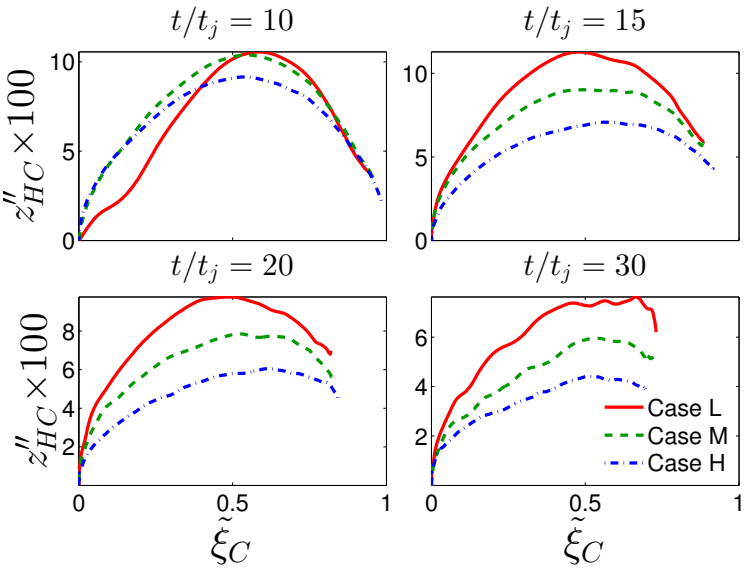

Figure 10: Comparison of z''_{HC}, defined in equation (6), against $\tilde{\xi}_C$ in the three CO/H_2 DNS flames, case L (solid lines), case M (dashed lines), and case H (dash-dotted lines), at $t/t_j = 10$, 15, 20, and 30.

3.1. Effect of Re on differential molecular diffusion in CO/H_2 DNS flames

Figure 9 compares $\tilde{z}_{HC}$ from the three CO/H_2 DNS flames at the different times. With the increase of Re, there is a clear trend of decrease of $\tilde{z}_{HC}$. This trend is consistent with

previous studies (e.g. [9][21]).

Figure 10 compares the rms z''_{HC}, defined in equation (6), in the CO/H_2 DNS flames case L, case M, and case H against $\tilde{\xi}_C$ at the different times. In all three CO/H_2 flames, z''_{HC} is zero at $\tilde{\xi}_C = 0$, increases to its peak value at about $\tilde{\xi}_C = 0.6$, and then decreases. When Re increases from case L ($Re_L = 2510$), to case M ($Re_M = 4478$), and then to case H ($Re_H = 9079$), we observe an overall trend of decreasing z''_{HC}, with the exception at $t/t_j = 10$ in case L. This exception is possibly caused by the equi-diffusion initial condition that is discussed in Section 2.1.

From Figures 9 and 10, we observe that both $\tilde{z}_{HC}$ and z''_{HC} have a strong dependence on Re, and when Re increases, both quantities tend to decrease. In the following section 3.2, we provide a quantitative analysis of this dependence.

3.2. Scaling analysis of differential molecular diffusion on Re

Bilger [9] pointed out that the level of the DMD effect scales as Re^{-1}. Here we provide an assessment of this scaling by using the CO/H_2 DNS flames. We quantify the level of the lumped effect of DMD in the CO/H_2 DNS flames by using the parameters $\widetilde{Z}_{HC}$ as defined in equation (5) and Z''_{HC} defined in equation (7). The values of $\widetilde{Z}_{HC}$ from the three CO/H_2 DNS flames are plotted against Re in Figure 11. In the figure, the collapse of the DNS results (shown as symbols) along a straight line in the log-log plot is excellent, indicating a scaling of $\widetilde{Z}_{HC} \sim Re^{-a}$, where a is a positive constant. The value of a depends on time t/t_j in the DNS flames and varies between 0.76 and 1.38 at the different times shown in the figure. This supports the scaling proposed by Bilger [9], although the exponent is not exactly -1 in the scaling.

Similarly, we examine the scaling of Z''_{HC} against Re in Figure 12. The results in the figure support a scaling of $Z''_{HC} \sim Re^{-a}$, where a is close to 0.5 except at time $t/t_j = 10$. This exception is likely caused by the effect of the equal diffusion initial condition in the DNS flames, as shown in Figure 5. In that figure it is seen that during the initial time (say $t/t_j < 10$), the value of $\widetilde{Z}_{HC}$ grows from zero (caused by the initial equi-diffusion effect) to a maximum. During this time, for the three cases (case L, case M, and case H), the relative

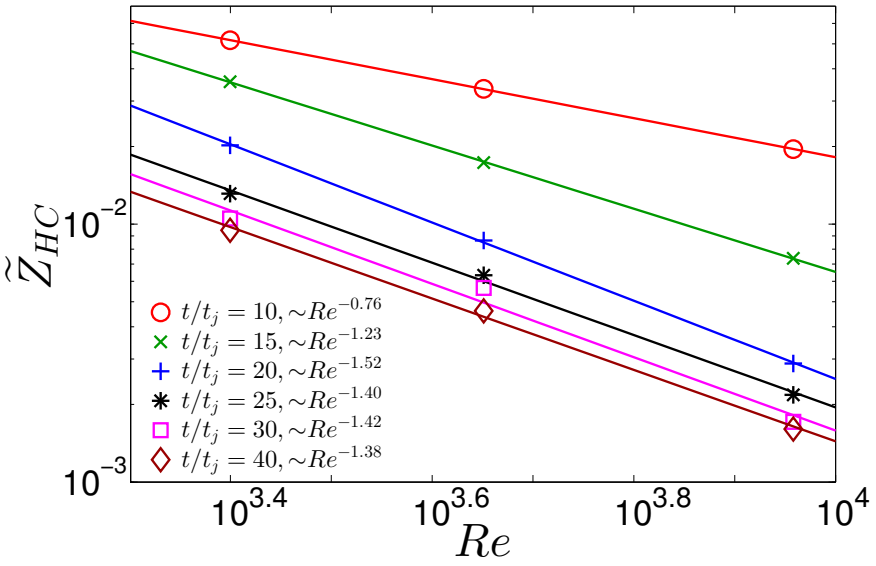

Figure 11: The scaling of $\widetilde{Z}_{HC}$ against Re in the three CO/H_2 DNS flames at t/t_j = 10, 15, 20, 25, 30, and 40. The solid lines are linear fits to the DNS results.

magnitudes of Z''_{HC} show an opposite trend compared to the later stage when $t/t_j > 10$, which results in the non-monotonic behavior of Z''_{HC} near $t/t_j = 10$ and the exception observed in Figure 12. Compared with the scaling found in Figure 12, a similar scaling for Z''_{HC} has been reported in the literature, e.g. [41], although contradicting observations have also been reported experimentally, e.g. in Smith et al. [31] where a non-monotonic effect of Re on z''_{HC} is observed in turbulent reacting jet flows. In an accompanying work, however, Smith et al. [34] reported scaling of z''_{HC} in a non-reacting jet and showed consistent scaling with the theory. It is generally expected that an accurate measurement of $\widetilde{z}_{HC}$ in the reacting jet is much more difficult although it is not clear exactly what is causing this inconsistency of scaling in the experiments. Further experimental effort is needed to reconcile the inconsistent observations. In the above scaling analysis, a single Re is used for each flame that is based on the global scales at the initial time. For non-reacting planar temporal mixing layer, self-similarity is observed [42] and hence the Re is a constant in time. Deviation from self-similarity occurs when combustion is present in the current DNS flames and hence the Re based on global scales changes in time. This deviation is small, and we have tried a time-dependent Re for the above scaling analysis as well, but did not observe

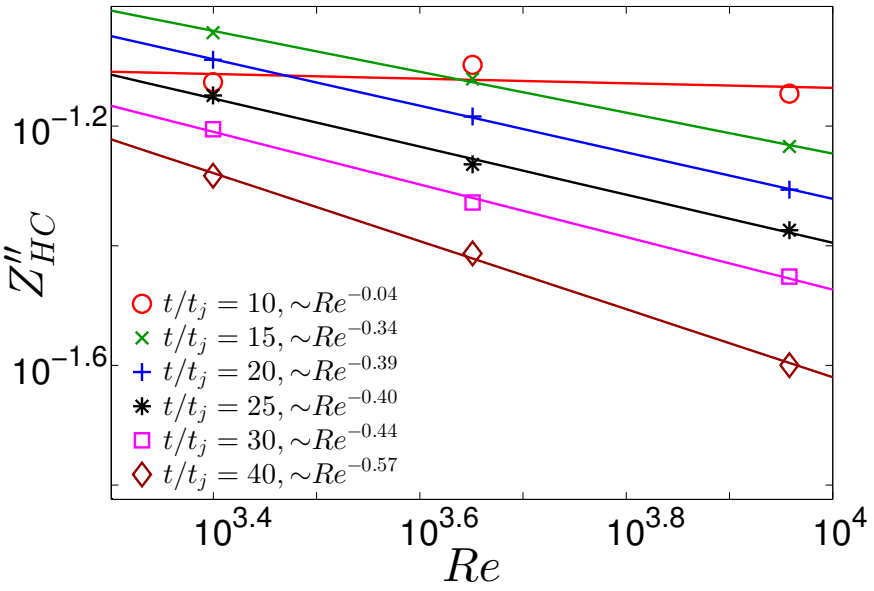

Figure 12: The scaling of Z''_{HC} against Re in the three CO/H_2 DNS flames at $t/t_j = 10$, 15, 20, 25, 30, and 40. The solid lines are linear fits to the DNS results.

any substantial difference in the scaling results.

To summarize, we examine the scaling of the effect of DMD in the three CO/H_2 DNS flames with increasing Re (and with fixed Da), in terms of $\widetilde{Z}_{HC}$ and Z''_{HC}. Both quantities are found to scale approximately as Re^{-a}, with a taken to be a positive constant. The value of a for $\widetilde{Z}_{HC}$ is close to 1.0, and the value of a for Z''_{HC} is close to 0.5. In the next Section 4, we further examine the scaling of the effect of DMD with respect to Da, through the analysis of both steady laminar C_2H_4 diffusion flamelets and the C_2H_4 DNS flames.

4. Dependence of differential molecular diffusion on *Da* number

In the C_2H_4 DNS flames, Re is fixed and Da is varied through a change to the fuel and oxidizer compositions so that the chemical reaction time scales are varied [30]. In the following, we first conduct a qualitative examination of the effect of DMD in the C_2H_4 DNS flames. Next we study the scaling of the effect of DMD against Da in a steady C_2H_4 laminar flamelet to provide a general understanding of the effect of Da on DMD. The scaling analysis is then extended to the C_2H_4 DNS flames to examine the effect of Da on DMD in turbulent

flames.

4.1. Effect of Da on differential molecular diffusion in C_2H_4 DNS flames

Figure 13 shows $\tilde{z}_{HC}$ against $\tilde{\xi}_C$ for the three C_2H_4 DNS flames. With a decrease of Da from case 1 to case 3, the magnitude of $\tilde{z}_{HC}$ decreases. The shape of the profiles of $\tilde{z}_{HC}$ from the different cases is very similar at the same time t/t_j. The location of the maximum $\tilde{z}_{HC}$ moves slightly to the fuel lean side when Da decreases. Figure 14 compares z''_{HC} against $\tilde{\xi}_C$ from the three C_2H_4 DNS cases. With a decrease of Da, the magnitude of z''_{HC} tends to decrease as well. There is one peak of z''_{HC} in the mixture fraction space. This peak location is different in time, and tends to move towards the oxidizer side as time increases. In the following Sections 4.2 and 4.3, we analyze the scaling dependence of the effect of DMD on Da.

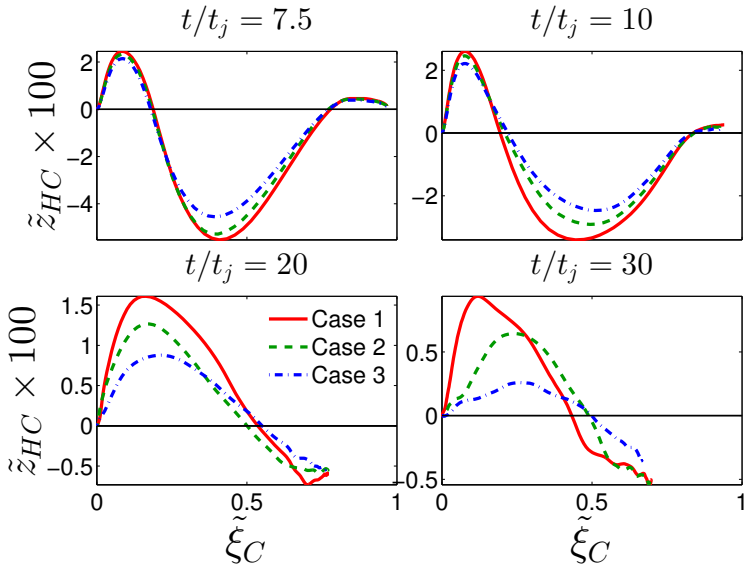

Figure 13: Comparison of $\tilde{z}_{HC}$ against $\tilde{\xi}_C$ in the three C_2H_4 DNS flames, case 1 (solid lines), case 2 (dashed lines), and case 3 (dash-dotted lines), at $t/t_j = 7.5$, 10, 20, and 30.

4.2. Scaling analysis of differential molecular diffusion on Da in a laminar flamelet

To gain deep insights into the effect of Da on DMD and its scaling, we design a series of laminar $C_2H_4/O_2/N_2$ diffusion flame test cases to examine the scaling of the effect of DMD

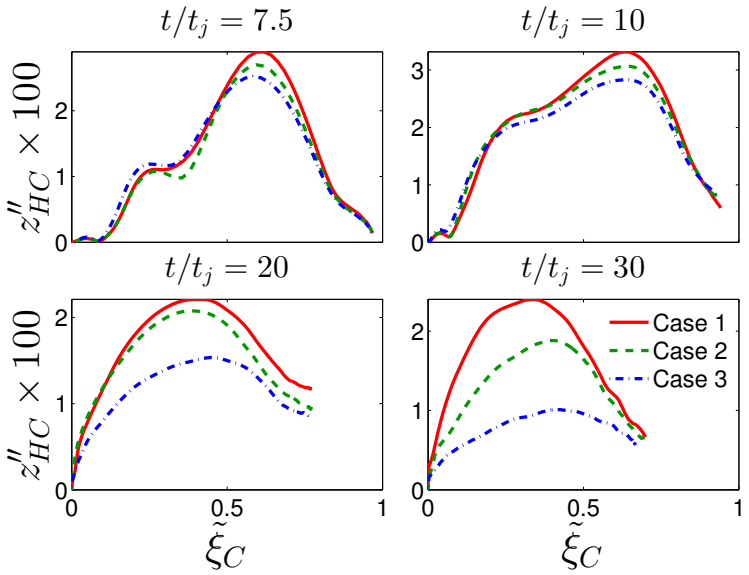

Figure 14: Comparison of z''_{HC} against $\tilde{\xi}_C$ in the three C_2H_4 DNS flames, case 1 (solid lines), case 2 (dashed lines), and case 3 (dash-dotted lines), at $t/t_j = 7.5$, 10, 20, and 30.

on Da in laminar non-premixed flames first, before we examine the scaling in the C_2H_4 DNS flames. We use counter-flow jet diffusion flames as the test cases [32] in which we vary Da by varying the chemical time scale while holding the flow time scale constant in order to have Re fixed, in a similar manner to the variation of Da in the DNS flames [30]. The flow time scale τ_f in the counter-flow jet flames scales as $\tau_f \sim a_s^{-1} \sim \chi_{st}^{-1}$ where a_s is the strain rate and χ_{st} is the scalar dissipation rate at the stoichiometric condition. The chemical time scale τ_c is proportional to $1/\chi_{st,q}$ [30], where $\chi_{st,q}$ is the extinction scalar dissipation rate. The Da number can then be defined as $Da = \tau_f/\tau_c = c_{Da}\chi_{st,q}/\chi_{st}$, where c_{Da} is a model constant and is chosen to be $c_{Da} = 1$. The change of $\chi_{st,q}$ can be achieved by varying the relative concentration of N_2 to fuel in the boundary values while keeping the stoichiometric condition to be the same [30]. In the tests, χ_{st} is specified to be always less than half of $\chi_{st,q}$, so that no extinction occurs. The Re number scales as $Re \sim u_f^2 \tau_f/\nu$, where u_f is the characteristic velocity and ν is the kinematic viscosity. In the test, u_f and τ_f are fixed and ν varies very slightly so that the Re number is approximately fixed while Da varies. When calculating Z_{HC} defined in equation (3) numerically, the discretization size of 0.005 in the mixture fraction space is used for the numerical integration.

The resultant Z_{HC} against Da in the laminar diffusion flames are shown in Figure 15. A multiple set of test cases are performed by varying χ_{st} (or the strain rate a_s) which is fixed for each set of test cases, i.e., Re is fixed for each set of test cases. Examining the same set of test cases, e.g., χ_{st} =36.7 s^{-1} (or a_s =100 s^{-1}) shown as the downward pointing triangles in Figure 15, it is readily observed that as Da decreases, Z_{HC} decreases, which is consistent with the C_2H_4 DNS flames shown in Figure 13. This trend of decreasing effect of DMD with decreasing Da can be explained by the limiting behaviors of the effect of DMD in the laminar flames. At a relatively small Da, extinction is likely to occur, and at extinction, there is no effect of DMD in the C_2H_4 flames in terms of the transport of elemental C and H. When Da is infinitely large, the chemistry is infinitely fast compared to the diffusion process, and hence the molecular diffusion is the controlling process. It is thus obvious that the effect of diffusion reaches its maximum effect when Da is largest in the present C_2H_4 flames, and so does the effect of DMD. Note, however, that the Da effect observed is with respect to moderate Re number DNS flames, and it remains to be seen whether, at sufficiently high Reynolds numbers, the Da effect is diminished.

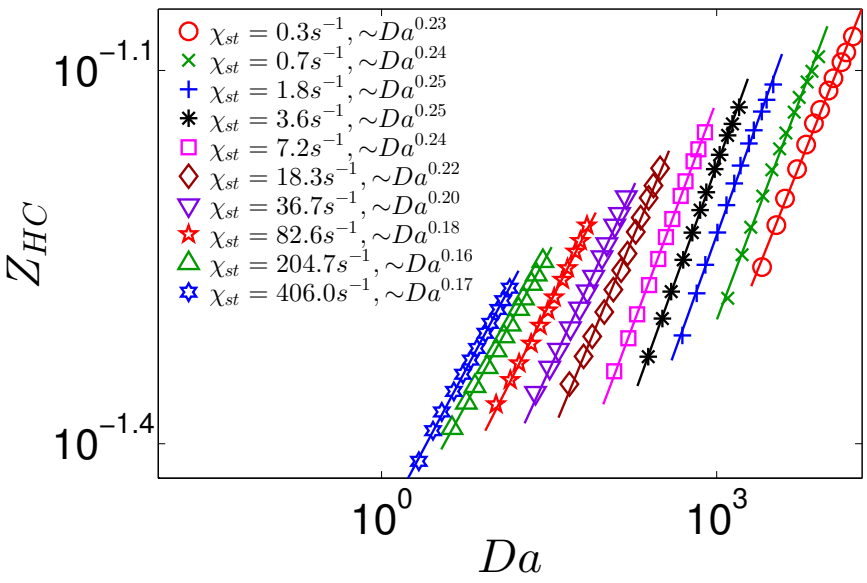

Figure 15: The scaling of Z_{HC} against Da in the $C_2H_4/O_2/N_2$ laminar diffusion flames computed from OPPDIF [32]. The solid lines are linear fits to the flame results.

For the same case of χ_{st} =36.7 s^{-1} (a_s =100 s^{-1}), another important observation from Figure 15 is that a clear scaling of $Z_{HC}{\sim}Da^{0.20}$ is observed. This scaling is confirmed by varying the strain rate (a_s or χ_{st}) for each set of test cases, as shown in Figure 15. With different values of χ_{st} ranging from 0.3 s^{-1} to 406 s^{-1} (or the strain rate ranging from 1 s^{-1} to 10^3 s^{-1}), a scaling of $Z_{HC}{\sim}Da^a$ (with a a positive constant) is strongly evident in all cases. The scaling exponent a is slightly different in each case with a different value of χ_{st} and is in the range of ($0.16 < a < 0.25$). The value of a is expected to be dependent on χ_{st} (or equivalently on the strain rate a_s). The results in Figure 15 suggest that when the rate of strain increases, the exponent a decreases, for a strain rate that is not too small, e.g. a_s >2 s^{-1} or χ_{st} >0.7 s^{-1}.

4.3. Scaling analysis of differential molecular diffusion on Da in C_2H_4 DNS flames

The scaling of the effect of DMD in the steady laminar diffusion flamelets in Section 4.2 provides insights into the effect of Da on DMD. We now examine the same scaling in the C_2H_4 DNS flames. The scaling of $\widetilde{Z}_{HC}$ against Da is explored in Figure 16. The results in the figure show a similar scaling to that in the laminar flames, $\widetilde{Z}_{HC}{\sim}Da^a$. Such a scaling is evident at the early times, $t/t_j{\leq}30$. For later times, it seems that there is some deviation from this scaling. An explanation for this is that case 3 involves significant extinction (see Figure 7) when $t/t_j{\geq}30$ [30], and the scaling we observed is likely not applicable to severe extinction. Another interesting observation that we can make from Figure 16 is that as time increases, the exponent a in the scaling also increases. It is noticed that when time increases in the C_2H_4 DNS flames, the characteristic rate of strain, U_m/L_m, where U_m is a characteristic velocity scale and L_m is the width of the mixing layer, decreases since L_m increases in time, since L_m scales as $\sqrt{t}$ and U_m scales as $1/\sqrt{t}$ in planar temporal mixing layer [42], and hence U_m/L_m scales as $1/t$. Therefore, in the DNS flames, as the characteristic rate of strain decreases, the exponent a in the DNS scaling increases. Apparently, this is consistent with the observations from the steady laminar flamelets in Section 4.2. This consistency provides support to the scaling observed in the DNS flames. It is worthwhile to point out that although we concluded that the effect of DMD in the C_2H_4 DNS flames

is non-flamelet-like in Section 2, the effect of Da on DMD seems to behave similarly in the DNS flames and in the steady laminar flamelets. This implies that the scaling we observed, Da^a, may be valid in turbulent C_2H_4 non-premixed flames over wide combustion regimes including both flamelet and non-flamelet regimes.

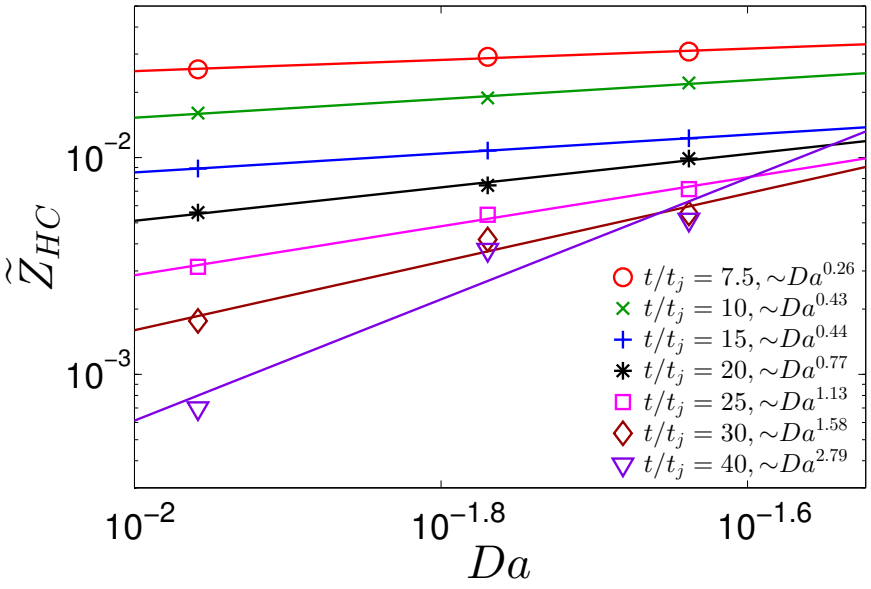

Figure 16: The scaling of $\widetilde{Z}_{HC}$ against Da in the three C_2H_4 DNS flames at $t/t_j = 7.5, 10$, 15, 20, 25, 30, and 40. The solid lines are linear fits to the DNS results.

In Figure 17, we further examine the scaling of Z''_{HC} against Da. A scaling of $Z''_{HC} \sim Da^a$, with a a positive constant, can also be clearly observed from the figure. At later times ($t/t_j \geq 30$), there is a slight deviation of the DNS results from this scaling, which is also a possible consequence of flame extinction for case 3 of the C_2H_4 DNS flames. Meanwhile, the exponent factor a appears to increase with time in the C_2H_4 DNS flames for Z''_{HC}, similar to that for $\widetilde{Z}_{HC}$.

5. Conclusions

In this work, two previously generated DNS datasets are interrogated extensively to extract qualitative and quantitative information about the effect of differential molecular diffusion (DMD) in turbulent non-premixed flames. The two DNS flames are in the same

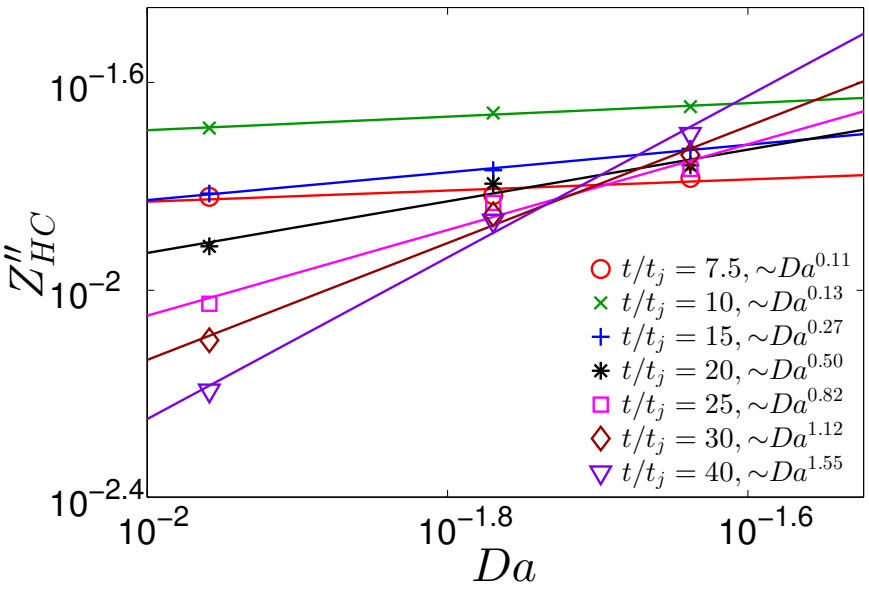

Figure 17: The scaling of Z''_{HC} against Da in the three C_2H_4 DNS flames at $t/t_j = 7.5, 10$, 15, 20, 25, 30, and 40. The solid lines are linear fits to the DNS results.

geometry: temporally evolving planar jet flames, and are performed with different fuels, one with CO/H_2 and the other with C_2H_4. In the CO/H_2 DNS flames, there are three cases with different Reynolds numbers Re, all with the same Da, and in the C_2H_4 flames, there are also three cases but with fixed Re, and with different Da. By exploring the DNS flames and comparing them with laminar diffusion flamelets, we are able to understand the qualitative difference of the two DNS flames, as well as the quantitative scaling of the effect of DMD against Re and Da. The following major conclusions can be drawn based on this study:

1. The effect of DMD in the CO/H_2 flames is found to be flamelet-like, i.e., it is similar to that in steady laminar diffusion flamelets;

2. The effect of DMD in the C_2H_4 flames is found to be flamelet-like during the early stage of the flames ($t/t_j \leq 10$) and becomes non-flamelet-like later;

3. In the CO/H_2 flames, it is found that the effect of DMD decreases when Re increases. An evident power law scaling is demonstrated for the effect of DMD in the CO/H_2 flames against Re;

4. In steady laminar diffusion flamelets, the effect of DMD increases when Da increases. Such a dependence of the effect of DMD on Da is described by a power law with excellent agreement;

5. The dependence of the effect of DMD on Da in the C_2H_4 DNS flames is found to be very similar to the dependence found in laminar diffusion flamelets, despite the fact that the DMD effect in C_2H_4 DNS flames is non-flamelet-like at later times. This suggests that the scaling found is probably valid in turbulent C_2H_4 non-premixed flames even if they are not in the flamelet regime.

Acknowledgments

Acknowledgment is made to the Donors of the American Chemical Society Petroleum Research Fund for support of this research. Evatt Hawkes is supported by the Australian Research Council. The work at Sandia was supported by the Division of Chemical Sciences, Geosciences and Bio-sciences, the Office of Basic Energy Sciences, the U.S. Department of Energy. Sandia National Laboratories is a multi-program laboratory operated by Sandia Corporation, a Lockheed Martin Company, for the U.S. Department of Energy under contract DE-AC04-94-AL85000.

References

[1] R. W. Bilger, Turbulent diffusion flames, Annu. Rev. Fluid Mech. 21 (1) (1989) 101–135.

[2] S. B. Pope, Turbulent Flows, Cambridge University Press, 2000.

[3] S. B. Pope, PDF methods for turbulent reactive flows, Prog. Energy Combust. Sci. 11 (2) (1985) 119–192.

[4] N. Peters, Laminar diffusion flamelet models in non-premixed turbulent combustion, Prog. Energy Combust. Sci. 10 (3) (1984) 319–339.

[5] R. J. Kee, M. E. Coltrin, P. Glarborg, Chemically reacting flow: theory and practice, John Wiley & Sons, 2005.

[6] R. Hilbert, F. Tap, H. El-Rabii, D. Thévenin, Impact of detailed chemistry and transport models on turbulent combustion simulations, Prog. Energy Combust. Sci. 30 (1) (2004) 61–117.

[7] C. Bruno, V. Sankaran, H. Kolla, J. H. Chen, Impact of multi-component diffusion in turbulent combustion using direct numerical simulations, Combust. Flame 162 (11) (2015) 4313–4330.

[8] H. A. Alrazen, A. A. Talib, R. Adnan, K. Ahmad, A review of the effect of hydrogen addition on the performance and emissions of the compression–ignition engine, Renew. Sust. Energ. Rev. 54 (2016) 785–796.

[9] R. W. Bilger, Molecular transport effects in turbulent diffusion flames at moderate Reynolds number, AIAA Journal 20 (7) (1982) 962–970.

[10] H. Wang, Consistent flamelet modeling of differential molecular diffusion for turbulent non-premixed flames, Phys. Fluids 28 (3) (2016) 035102.

[11] C. K. Law, Combustion physics, Cambridge university press, 2010.

[12] P. J. Goix, I. Shepherd, Lewis number effects on turbulent premixed flame structure, Combust. Sci. Technol. 91 (4-6) (1993) 191–206.

[13] R. G. Abdel-Gayed, D. Bradley, M. Lawes, Turbulent burning velocities: a general correlation in terms of straining rates, Proc. R. Soc. Lond. A 414 (1847) (1987) 389–413.

[14] D. C. Haworth, T. J. Poinsot, Numerical simulations of Lewis number effects in turbulent premixed flames, J. Fluid Mech. 244 (1992) 405–436.

[15] W. T. Ashurst, N. Peters, M. Smooke, Numerical simulation of turbulent flame structure with non-unity Lewis number, Combust. Sci. Technol. 53 (4-6) (1987) 339–375.

[16] D. H. Rowinski, S. B. Pope, Computational study of lean premixed turbulent flames using RANS/PDF and LES/PDF methods, Combust. Theory Modelling 17 (4) (2013) 610–656.

[17] S. Viswanathan, S. B. Pope, Turbulent dispersion from line sources in grid turbulence, Phys. Fluids 20 (10) (2008) 101514.

[18] K. A. Kemenov, S. B. Pope, Molecular diffusion effects in LES of a piloted methane–air flame, Combust. Flame 158 (2) (2011) 240–254.

[19] H. Wang, K. Kim, Effect of molecular transport on PDF modeling of turbulent non-premixed flames, Proc. Combust. Inst. 35 (2) (2015) 1137–1145.

[20] J. C. Sutherland, P. J. Smith, J. H. Chen, Quantification of differential diffusion in nonpremixed systems, Combust. Theory Modelling 9 (2) (2005) 365–383.

[21] R. S. Barlow, J. H. Frank, A. N. Karpetis, J.-Y. Chen, Piloted methane/air jet flames: Transport effects and aspects of scalar structure, Combust. flame 143 (4) (2005) 433–449.

[22] H. Pitsch, Unsteady flamelet modeling of differential diffusion in turbulent jet diffusion flames, Combust. Flame 123 (3) (2000) 358–374.

[23] V. Gopalakrishnan, J. Abraham, Effects of multicomponent diffusion on predicted ignition characteristics of an n-heptane diffusion flame, Combust. Flame 136 (4) (2004) 557–566.

[24] R. Hilbert, D. Thévenin, Influence of differential diffusion on maximum flame temperature in turbulent nonpremixed hydrogen/air flames, Combust. flame 138 (1) (2004) 175–187.

[25] Y. Chen, J.-Y. Chen, Fuel-dilution effect on differential molecular diffusion in laminar hydrogen diffusion flames, Combust. Theory Modelling 2 (4) (1998) 497–514.

[26] Y. Minamoto, H. Kolla, R. W. Grout, A. Gruber, J. H. Chen, Effect of fuel composition and differential diffusion on flame stabilization in reacting syngas jets in turbulent cross-flow, Combust. Flame 162 (10) (2015) 3569–3579.

[27] B. M. G. Maragkos, P. Rauwoens, Assessment of a methodology to include differential diffusion in numerical simulations of a turbulent flame, Int. J. Hydrogen Energy 40 (2) (2015) 1212–1228.

[28] M. Z. J. Jiang, X. Jiang, A computational study of preferential diffusion and scalar transport in nonpremixed hydrogen-air flames, Int. J. Hydrogen Energy 40 (45) (2015) 15709–15722.

[29] E. R. Hawkes, R. Sankaran, J. C. Sutherland, J. H. Chen, Scalar mixing in direct numerical simulations of temporally evolving plane jet flames with skeletal CO/H_2 kinetics, Proc. Combust. Inst. 31 (1) (2007) 1633–1640.

[30] D. O. Lignell, J. H. Chen, H. A. Schmutz, Effects of Damköhler number on flame extinction and reignition in turbulent non-premixed flames using DNS, Combust. Flame 158 (5) (2011) 949–963.

[31] L. L. Smith, R. W. Dibble, L. Talbot, R. S. Barlow, C. D. Carter, Laser Raman scattering measurements of differential molecular diffusion in turbulent nonpremixed jet flames of H_2/CO_2 fuel, Combust. flame 100 (1) (1995) 153–160.

[32] A. E. Lutz, R. J. Kee, J. F. Grcar, F. M. Rupley, OPPDIF: A fortran program for computing opposed-flow diffusion flames, Sandia National Laboratories, Albuquerque, New Mexico, No. SAND96-8243, 1996.

[33] R. W. Dibble, M. B. Long, Investigation of differential diffusion in turbulent jet flows using planar laser Rayleigh scattering, Combust. Flame 143 (4) (2005) 644–649.

[34] L. L. Smith, R. W. Dibble, L. Talbot, R. S. Barlow, C. D. Carter, Laser Raman scattering measurements of differential molecular diffusion in nonreacting turbulent jets of H_2/CO_2 mixing with air, Phys. Fluids 7 (6) (1995) 1455–1466.

[35] W. Meier, S. Prucker, M.-H. Cao, W. Stricker, Characterization of turbulent H_2/N_2/Air jet diffusion flames by single-pulse spontaneous Raman scattering, Combust. Sci. Technol. 118 (4-6) (1996) 293–312.

[36] R. S. Barlow, G. J. Fiechtner, C. D. Carter, J.-Y. Chen, Experiments on the scalar structure of turbulent $CO/H_2/N_2$ jet flames, Combust. Flame 120 (4) (2000) 549–569.

[37] R. S. Barlow, M. J. Dunn, M. S. Sweeney, S. Hochgreb, Effects of preferential transport in turbulent bluff-body-stabilized lean premixed CH_4/air flames, Combust. Flame 159 (8) (2012) 2563–2575.

[38] H. Pitsch, N. Peters, A consistent flamelet formulation for non-premixed combustion considering dif-

ferential diffusion effects, Combust. Flame 114 (1) (1998) 26–40.

[39] C. Han, D. Lignell, E. Hawkes, J. H. Chen, H. Wang, Flamelet modeling of differential molecular diffusion in CO/H_2 and ethylene DNS flames, in: APS Division of Fluid Dynamics Meeting, Boston, Massachusetts, 2015.

[40] J. Xu, S. B. Pope, PDF calculations of turbulent nonpremixed flames with local extinction, Combustion and Flame 123 (3) (2000) 281–307.

[41] A. Kerstein, M. Cremer, P. McMurtry, Scaling properties of differential molecular diffusion effects in turbulence, Phys. Fluids 7 (8) (1995) 1999–2007.

[42] G. K. Batchelor, An introduction to fluid dynamics, Cambridge University Press, 2000.